Available online at www.sciencedirect.com
ScienceDirect
International Journal of Mechanical Sciences 49 (2007) 335–351
International Journal of MECHANICAL SCIENCES
www.elsevier.com/locate/ijmecsci

Upper bound analysis for extrusion at various die land lengths and shaped profiles

J.S. Ajiboye[a,*], M.B. Adeyemi[b]

[a]Department of Mechanical Engineering, University of Lagos, Lagos, Nigeria
[b]Department of Mechanical Engineering, University of Ilorin, Ilorin, Nigeria

Received 2 August 2006; accepted 13 August 2006
Available online 6 October 2006

Abstract

The effects of die land lengths, a rarely investigated die extrusion parameter on the die-shaped profiles, on the extrusion pressures are investigated and presented. The analyses of the extrusion pressures by the upper bound method have been extended for the evaluations of the extrusion pressures to complex extruded sections such as square, rectangular, I,- and T-shaped sections with power of deformation due to ironing effect at the die land taken into account. The extrusion pressure contributions due to the die land evaluated theoretically for shaped sections considered are found to increase with die land lengths for any given percentage reduction and also increase with increasing percentage die reductions at any given die land length. The effect of die land lengths on the extrusion pressure increases with increasing complexity of die openings geometry with I-shaped section giving the highest extrusion pressure followed by T-shaped section, rectangular, circular-shaped die openings with square section die opening, giving the least extrusion pressure for any given die reduction at any given die land lengths.

Keywords: Extrusion pressures; Die land; Shaped sections; %reduction in area; Area ratio

1. Introduction

Upper bound solution provides an over estimation of the required deformation force, so many researchers have used this method of analysis to examine the influences of some deforming parameters on the working pressures involved in metal working operations. With regards to the three-dimensional extrusion of shaped sections, some analytical methods for predicting the metal flows under optimum die configurations have been proposed and analyzed [1]. In a study, on extrusion of non-symmetric T-shaped sections and their positioning, Chitkara and Celik [2] found that positioning of T-section not only affect considerably the required extrusion pressure, but vary the curvature and the quality of the extruded product. They pointed out that even where horizontal extrusion machines are used, for the axisymmetric extrusion the extruded product may come out bent due to the increased frictional resistance at the bottom part of the billet. To correct this, in practice sufficient lengths of die land are usually added to the die to achieve straight products. The curvature increases, as the friction factor m, increases. However, it is likely that the curvature of the exiting product depends not only on the frictional condition, but also on the surface geometry, die land length, the reduction in area, as well as the location and the shape of the cross-section vis-à-vis the original billet cross-section. Chitkara and Yohngjo [3] used integration to predict the energy expressions obtained from velocity field by upper bound method to analyze the deforming load and the deformed configurations. In another study, Chitkara and Yohngjo [4], predicted the upper bound load and the deformed configurations by the velocity field at varying punch movements and varying friction factors. The predicted forging load and the dimensionless forging pressures are found to be in good agreement with the experimental results. Wu and Hsu [5]

*Corresponding author.
E-mail address: joesehinde@yahoo.com (J.S. Ajiboye).

0020-7403/$ - see front matter © 2006 Elsevier Ltd. All rights reserved.
doi:10.1016/j.ijmecsci.2006.08.017

Nomenclature

P^*	total power of deformation
W_i	internal strain rate power of deformation
W_f	frictional power losses
W_s	shear power dissipated at boundaries of velocity discontinuity
σ_o	flow stress of the working material
r, φ, y	cylindrical coordinate
V_o	steady punch velocity
V_r, V_y, V_φ	velocity components
$r_s(\varphi, y)$	functions defining the shape of die geometry
$\varphi_f(y)$	function defining the zone of plastic deformation
$\dot{\varepsilon}_{ii}$, $\dot{\varepsilon}_{ij}$	strain rate components
m	friction coefficient or factor
P_{ave}	average punch pressure
Δv	resultant velocity or relative velocity slip
H_o	original billet height
y_1	die length
R	% reduction in area
r_o	radius of circular billet
2α	included die angle
x	die land length
D_o	original billet diameter
P_{max}, P_{min}, P'	extrusion pressures
Y	mean yield stress
ε	true strain
$\omega(\phi, y)$	angular velocity
y'	current billet height to die surface
A_o	original billet area
Γ_s	boundaries of velocity discontinuity at exit, entry including singular points
A_2	Billet area responsible for the web
A_1	Billet area responsible for the flange
a, b	height, length of sides of rectangle section
A_2/A_1	area ratio
L	die length

presented a model based on upper bound theorem to analyze the extrusion of composite clad rods with non-axisymmetric cross-section. Choi et al. [6] proposed upper bound analysis for the guiding and clamping-type forging of helical gears. Kar and Das [7] presented a study using SERR (spatial elementary rigid regions) based on upper bound analysis to analyse extrusion of I-section bars from square/rectangular billets. Celik and Chitkara [8] developed a computer program to obtain optimum die design which yields the lowest upper-bound load for a given reduction in area, die length, off-centric positioning and frictional conditions. Chitkara and Bhutta [9] estimated forging die loads from the mechanics of the process analyzed, using mixed cylindrical and Cartesian coordinate systems. Bae et al. [10] proposed a velocity field, based on upper bound analysis, for the prediction of the extrusion load in the square-die forward extrusion of circular-shaped bars from regular polygonal billets. Maity et al. [11] proposed an upper bound analysis, derived from a kinematically-admissible velocity fields using a dual-stream-function technique, for the extrusion of square sections from square billets through curved dies with prescribed profiles. Qamar et al. [12] conducted series of experiments using dies of different complexity to track the effects of ram speed variation and changing die profiles on extrusion pressure using Al-6063, the most commercial variety of structural aluminum. Chitkara and Adeyemi [13] examined in details both the deformation modes and the internal flow patterns of the deformed specimens to ascertain the metal flow patterns in the production of shaped sections such as I and T sections. The effect of reduction in area in extruding such shaped sections on the extrusion pressure was empirically determined. From their investigations, it was found that for any reduction in area of the I- and T-shaped sections, the extrusion pressures were greater when extruded from circular billets than when from square billets. Both MacLellan [14] and Wistreich [15] neglected the parallel portion or die land during their investigations on wire drawing operations though they thought it was important to include. In the theoretical equation of drawing stresses derived by Sach et al. [16], the die land was also neglected. Yang [17], using Sach's approach, derived a theoretical equation for rod drawing operations which included the effect of the land and comparison of the values of friction coefficients from both calculations; including and neglecting die land were made. The differences between the friction coefficients calculated with and without the land were found to be appreciable and hence concluded that the inclusion of die land effects in both the theoretical and experimental analyses. Kiuchi et al. [18] developed an upper bound based analytical method to calculate power requirements, the extrusion pressure, the optimal die length in extruding/drawing from round, square and rectangular billets to rods, bars and wires with square, rectangular, hexagonal, L-type, T-type, H-type and flower-type cross-sections. For this generalized formulation, it also has the setback for neglecting to account for the frictional forces at the die land region. Nanhai et al. [19] stressed the importance of proper simulation of die land in the extrusion of shapes with flat-faced die so as to avoid the generations of geometrical defects and hence proposed a method of simulation, using finite element method, that the metal flow in extrusion and the die land can be adjusted according to the simulation results. Ajiboye and Adeyemi [20] based on Kiuchi et al.'s [18] approach extended and improved their analytical method by taking into account effects of die-entrance angles, frictional powers at punch-material and chamber material interfaces to frictional die surface to study the effects of die reductions, billet shapes, die opening's geometrical shapes, surface conditions and dimensional ratios of rectangle die openings on the extrusion pressures of forward extrusion operations.

Avitzur [21] gave a detailed theoretical formulation which accounted for the power losses due to friction between the die land and round billets during drawing and extrusion processes to smaller rod products. He concluded that an increase in die land led into increase in the required force and decreased in maximum possible reductions. Ajiboye and Adeyemi [22] improved their previous formulations [20] to account for power losses due to ironing effect at the die land of an extrusion die with circular die opening. Their investigations involved the determinations of both experimental and theoretical effects of die land lengths on the quality of extruded products, extrusion pressures and flow patterns of cold-extruded lead alloy of circular sections. In the present study, the upper bound method of analysis of the effects of die land lengths on the extrusion pressures are formulated and extended to evaluate the extrusion pressures for complex extruded sections such as square, rectangular, I- and T-shaped sections with the powers of deformations due to ironing effect at die land taken into account. The effects of the die land lengths, die opening profiles and percentages reductions in areas on the extrusion pressure contributions due to die land effects are also investigated theoretically and presented.

2. Theoretical analysis

2.1. Velocity fields

A generalized shape of the die used in the analysis is shown in Fig. 1(a). The figure shows the shape of die surface expressed [18,20] by a function $r_s(\varphi, y)$ in cylindrical coordinate system. If the profile of the exit cross-section of the die is expressed by a function $\zeta(\varphi)$, the shape of the die surface, $r_s(\varphi, y)$ can then be expressed as

$$r_s(\varphi, y) = \frac{\zeta(\varphi) - r_0}{y_1} y + r_0, \tag{1}$$

where r_o is the radius of the round billet and y_1 is the length of the die. By using Eq. (1), and the function $r_s(\varphi, y)$, all of the strain rate components and the total powers of deformation can be calculated.

The boundary limits for the die surfaces are:

$$\begin{aligned} 0 \leqslant r \leqslant r_s(\varphi, y), \\ 0 \leqslant \varphi \leqslant \varphi_f(y), \\ 0 \leqslant y \leqslant y_1. \end{aligned} \tag{2}$$

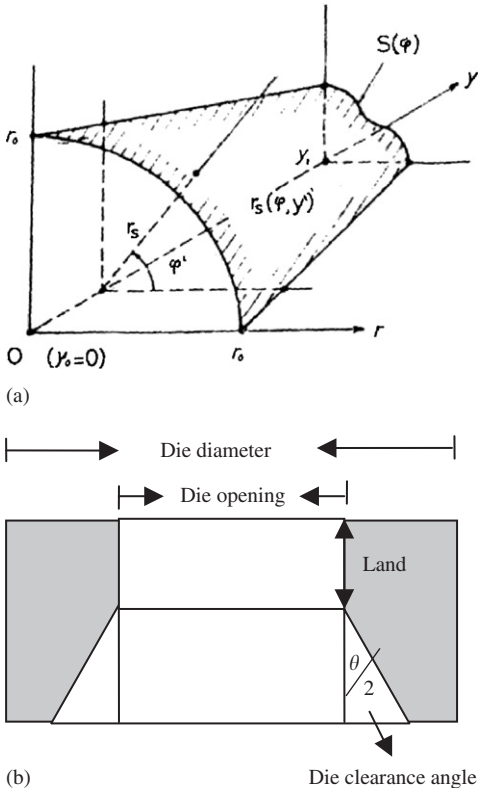

Fig. 1. (a) Shape and dimension of the linearly converging die employed in numerical calculations. (b) Die configurations.

2.1.1. Assumptions

The following assumptions [18,20] are used;

i. The longitudinal velocity, $V_{y,}$ is uniform at each cross-section of the material in the die and is equal to inlet velocity denoted by V_o at the entry.
ii. The Von-Mises yield criterion is assumed to be applicable.
iii. The rotational velocity component $V_\varphi(r, \varphi, y)$ is expressed as a product of two functions as follows:

$$V_\varphi(r, \varphi, y) = r \cdot w(\varphi, y) \tag{3}$$

iv. The rotational velocity component is given as $V_\varphi(r, \varphi_f(y), y)$ at the boundary defined by the function $\varphi_f(y)$, the plastic zone spreads in the direction from the boundary denoted by $\varphi_f(0)$ to the boundary denoted by $\varphi_f(y)$.

The generalized formulae of the kinematically admissible velocity field can be formulated as follows:
From the continuity equation we have

$$\varepsilon_r + \varepsilon_\varphi + \varepsilon_y = 0, \tag{4}$$

that is

$$\frac{\partial V_r(r, \varphi, y)}{\partial r} + \frac{1}{r} V_r(r, \varphi, y) + \frac{\partial V_y(r, \varphi, y)}{\partial y} + \frac{1}{r}\frac{\partial V_\varphi(r, \varphi, y)}{\partial \varphi} = 0. \tag{5}$$

From the assumption that the longitudinal velocity component V_y is uniform at each cross-section of the material in the die, employing condition of volume constancy, we have

$$V_y(y) \int_0^{\varphi_f(y)} r_s^2(\varphi, y)\, \mathrm{d}\varphi = V_0 \int_0^{\varphi_f(0)} r_s^2(\varphi, 0)\, \mathrm{d}\varphi,$$

which then gives

$$V_y(v) = \frac{V_0 \int_0^{\varphi(0)} r_s^2(\varphi, 0)\, \mathrm{d}\phi}{\int_0^{\varphi(y)} r_s^2(\varphi, y)\, \mathrm{d}\varphi}. \tag{6}$$

Multiply Eq. (5) by r, collect like terms, integrate both sides and noting that the boundary condition that when $r = 0$, V_r should be zero, we have

$$V_r(r, \varphi, y) = \frac{1}{r} \int_0^r r \left[\frac{\partial V_y(y)}{\mathrm{d}y} + \frac{1}{r}\frac{\partial V_\varphi(r, \varphi, y)}{\partial \phi} \right] \mathrm{d}r. \tag{7}$$

Assuming that the material flow along the shape of die, and noting that $V_\varphi = 0$ when $\varphi = 0$, the next velocity component is derived thus;

$$V_\varphi(r, \varphi, y) = \frac{r}{r_s^2(\varphi, y)} \int_0^\varphi \frac{\partial}{\partial y} \left[V_y(y) r_s^2(\varphi, y) \right] \mathrm{d}\varphi. \tag{8}$$

Eqs. (6)–(8) satisfy condition of volume constancy and all the kinematic boundary conditions and are, hence, refers to as the kinematically admissible velocity fields.

2.2. Strain rates and powers of deformation

The strain rate components are defined based on kinematically admissible velocity fields of Eqs. (6)–(8) as follows:

$$\dot{\varepsilon}_{rr}(\varphi, y) = \frac{1}{2} \left[\frac{\partial \omega(\varphi, y)}{\partial \varphi} + \frac{\partial V_y(y)}{\partial y} \right], \tag{9}$$

$$\dot{\varepsilon}_{\varphi\varphi}(\varphi, y) = \frac{1}{2} \left[\frac{\partial \omega(\varphi, y)}{\partial \varphi} - \frac{\partial V_y(y)}{\partial y} \right], \tag{10}$$

$$\dot{\varepsilon}_{yy}(y) = \frac{\partial V_y(y)}{\partial y}, \tag{11}$$

$$\dot{\varepsilon}_{r\varphi}(\varphi, y) = -\frac{1}{4}\frac{\partial \omega(\varphi, y)}{\partial^2 \varphi}, \tag{12}$$

$$\dot{\varepsilon}_{\varphi y}(r,\varphi,y)=\frac{r}{2}\frac{\partial\omega(\varphi,y)}{\partial y}, \tag{13}$$

$$\dot{\varepsilon}_{yr}(r,\varphi,y)=\frac{r}{4}\left[\frac{\partial^2\omega(\varphi,y)}{\partial y\partial\varphi}+\frac{\partial^2 Vy}{\partial y^2}\right]. \tag{14}$$

The internal power of deformation W_i is, therefore, defined as,

$$W_i=\sigma_0\iiint\sqrt{\frac{2}{3}\left(\dot{\varepsilon}_{rr}^2+\dot{\varepsilon}_{\varphi\varphi}^2+\dot{\varepsilon}_{yy}^2+2\left\{\dot{\varepsilon}_{r\varphi}^2+\dot{\varepsilon}_{y\varphi}^2+\dot{\varepsilon}_{yr}^2\right\}\right)}r\,\mathrm{d}r\,\mathrm{d}\varphi\,\mathrm{d}y. \tag{15}$$

The shear loss, $W_{s'}$ is given by

$$W_s=\int_{\Gamma s}\frac{\bar{\sigma}_0}{\sqrt{3}}(\Delta V)\Gamma_s\,\mathrm{d}s, \tag{16}$$

where

$$(\Delta V)\Gamma_s=\sqrt{\left[V_\varphi^2(r,\varphi,y^*)+V_r^2(r,\varphi,y^*)\right]} \tag{17}$$

The relative slip on the internal boundaries of velocity discontinuity is expressed by

$$\Delta V_r=\left|\left|-\frac{r}{2}\left[\frac{\partial\omega(\varphi+0,y)}{\partial\varphi}-\frac{\partial\omega(\varphi-0,y)}{\partial\varphi}\right]\right|\right|. \tag{18}$$

Using the concept of friction factor, the frictional power dissipated at the punch/material interface is given by:

$$W_{f_1}=\frac{m\sigma_0}{\sqrt{3}}\int_0^{r0}\int_0^{2\pi}|V_r|r\,\mathrm{d}\varphi\,\mathrm{d}y, \tag{19}$$

where $V_r=$ radial velocity, given as

$$V_r(\varphi,r,y)=-\frac{r}{2}\left[\frac{\partial V_y(y)}{\partial y}+\frac{\partial\omega(\varphi,y)}{\partial\varphi}\right], \tag{20}$$

where

$$V_y(y)=\left(\frac{y}{H_0-y'}\right)\frac{V_0\int_0^{\varphi_f(0)}r_s^2(\varphi,0)\,\mathrm{d}\varphi}{\int_0^{\varphi_f(y)}r_s^2(\varphi,y)\,\mathrm{d}\varphi}, \tag{21}$$

where H_0 is initial billet height, y' is current billet height to die surface and σ_0 is the mean yield stress and y is an instantaneous position along the axis.

The frictional power, W_{f2} between work–material/die cylindrical surfaces, due to relative axial sliding velocity at radius, r_o is given by

$$W_{f2}=\frac{m\sigma_0}{\sqrt{3}}\int_0^{(H_0-y')}\int_0^{2\pi}\left|V_y(y)\right|r\,\mathrm{d}\varphi\,\mathrm{d}y. \tag{22}$$

2.3. Frictional power at die land

As reported earlier, most of the previous works, apart from that of Yang [17] and Avitzur [21], which was of course limited to simple geometry of round billet to smaller rods, the contribution of frictional power at die land to the entire deformation load is usually neglected. The present formulation [23] based on upper bound analysis accounts for frictional power at the die land (see Fig. 1(b) for details of extrusion die configurations) and for various die opening shapes, namely square, rectangular, I- and T-shaped sections. The axial velocity is modified using condition of volume constancy between the inlet and the die land region as follows. (Figs. 2–5).

The frictional powers at the die land, for shaped sections, such as rectangular, square, T- and I-sections are formulated as follows.

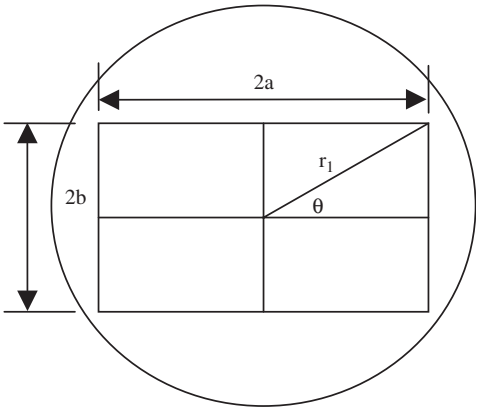

Fig. 2. Rectangular die opening.

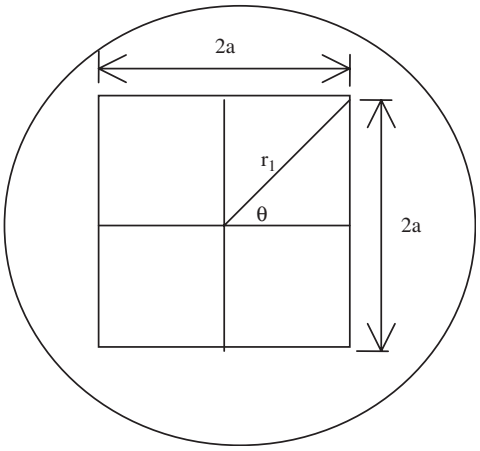

Fig. 3. Square die opening.

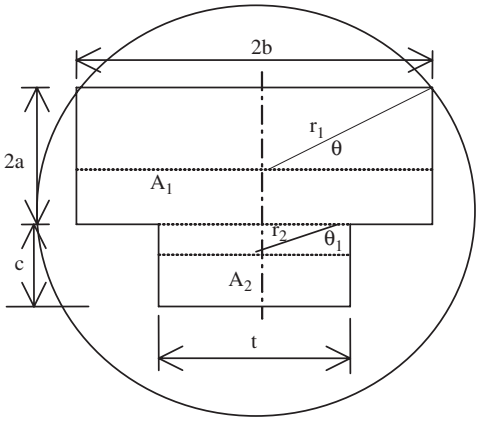

Fig. 4. T-shaped die opening.

2.3.1. Rectangular die opening (where $r_1 = \sqrt{(a^2 + b^2)}$ *and* $\theta = \tan^{-1} b/a$*)*

$$Wf_{\text{land}} = \frac{4m\sigma_0}{\sqrt{3}} \left[\int_0^x \int_0^\theta V_y(y) r_1 \, \mathrm{d}\varphi \, \mathrm{d}y + \int_0^x \int_0^{((\pi/2)-\theta)} V_y(y) r_1 \, \mathrm{d}\varphi \, \mathrm{d}y \right], \tag{23}$$

where applying volume constancy between the entry and the land

$$V_y(y) = \frac{2\pi}{(1-R)\sin 2\theta} \frac{\int_0^{\varphi(0)} r_s^2(\varphi, 0) \, \mathrm{d}\varphi}{\int_0^{\varphi(y)} r_s^2(\varphi, y) \, \mathrm{d}\varphi}, \quad \text{where} \quad \pi/4 < \theta > \pi/4. \tag{24}$$

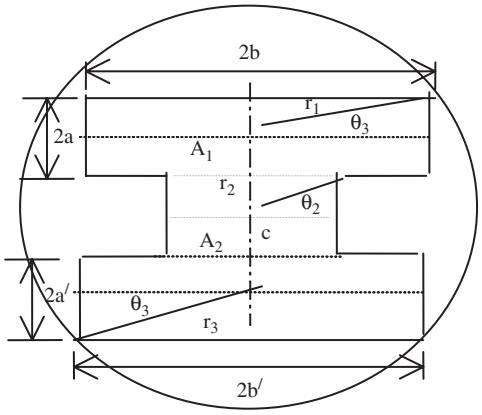

Fig. 5. I-shaped die opening.

2.3.2. Square die opening ($\theta = \pi/4$)

$$Wf_{\text{land}} = \frac{8m\sigma_0}{\sqrt{3}}\left[\int_0^x \int_0^{\pi/4} V_y(y) r_1 \, \mathrm{d}\phi \, \mathrm{d}y\right], \tag{25}$$

where, applying volume constancy between the entry and the land,

$$V_y(y) = \frac{\pi}{(1-R)\sin^2\theta} \frac{\int_0^{\varphi(0)} r_s^2(\varphi, 0)\, \mathrm{d}\varphi}{\int_0^{\varphi(y)} r_s^2(\varphi, y)\, \mathrm{d}\varphi}, \tag{26}$$

2.3.3. T-shaped die opening

$$Wf_{\text{land}} = \frac{2m\sigma_o}{\sqrt{3}}\begin{bmatrix} 4\left[\int_0^x \int_0^{\theta} V_y(y) r_1 \, \mathrm{d}\varphi \, \mathrm{d}y + \int_0^x \int_0^{(\pi/2)-\theta} V_y(y) r_1 \, \mathrm{d}\varphi \, \mathrm{d}y\right] - 2\langle \int_0^x \int_0^{\pi/2-\theta_1} V_y(y) r_2 \, \mathrm{d}\varphi \, \mathrm{d}y\rangle \\ +2\left\{\int_0^x \int_0^{\theta_1} V_y(y) r_2 \, \mathrm{d}\varphi \, \mathrm{d}y + \int_0^x \int_0^{(\pi/2)-\theta_1} V_y(y) r_2 \, \mathrm{d}\varphi \, \mathrm{d}y\right\} + 2\left(\int_0^x \int_0^{\theta_1} V_y(y) r_2 \, \mathrm{d}\varphi \, \mathrm{d}y\right) \end{bmatrix} \tag{27}$$

where,

$$r_1 = \sqrt{(a^2 + b^2)},\ \theta_1 = \tan^{-1} a/b,$$
$$r_2 = \sqrt{(t/2)^2 + (c/2)^2},\ \theta_2 = \tan^{-1} c/t.$$

2.3.4. I-shaped die opening

$$Wf_{\text{land}} = \frac{4m\sigma_o}{\sqrt{3}}\begin{bmatrix} 4\left\{\int_0^x \int_0^{\theta_1} V_y(y) r_1 \, \mathrm{d}\varphi \, \mathrm{d}y + \int_0^x \int_0^{(\pi/2)-\theta_1} V_y(y) r_1 \, \mathrm{d}\varphi \, \mathrm{d}y\right\} - 2\langle \int_0^x \int_0^{\pi/2-\theta_2} V_y(y) r_2 \, \mathrm{d}\varphi \, \mathrm{d}y\rangle \\ +4\left(\int_0^x \int_0^{\theta_2} V_y(y) r_2 \, \mathrm{d}\varphi \, \mathrm{d}y\right) + 4\left\{\int_0^x \int_0^{\theta_3} V_y(y) r_3 \, \mathrm{d}\varphi \, \mathrm{d}y + \int_0^x \int_0^{(\pi/2)-\theta_3} V_y(y) r_3 \, \mathrm{d}\varphi \, \mathrm{d}y\right\} \\ -2\left[\int_0^x \int_0^{(\pi/2)-\theta_2} V_y(y) r_3 \, \mathrm{d}\varphi \, \mathrm{d}y\right] \end{bmatrix}, \tag{28}$$

where,

$$r_1 = \sqrt{(a^2 + b^2)},\ \theta_1 = \tan^{-1} a/b,$$
$$r_2 = \sqrt{(t/2)^2 + (c/2)^2},\ \theta_2 = \tan^{-1} c/t,$$
$$r_3 = \sqrt{\left(a'^2 + b'^2\right)},\ \theta_3 = \tan^{-1} a'/b',$$

where, applying volume constancy between the entry and the land, for both T- and I-sections, we have

$$V_y(y) = \frac{2\pi}{(1-R)\sin 2\theta} \frac{\int_0^{\varphi(0)} r_s^2(\varphi, 0)\,\mathrm{d}\varphi}{\int_0^{\varphi(y)} r_s^2(\varphi, y)\,\mathrm{d}\varphi}, \quad \text{where} \quad \pi/4 < \theta > \pi/4. \tag{29}$$

Therefore, the total frictional power ΣW_f is given by

$$\sum W_f = W_{f_1} + W_{f_2} + W_{f_{\text{land}}}. \tag{30}$$

Therefore, the total powers of deformation, P^* is obtained, using

$$P^* = W_i + \sum W_s + \sum W_f. \tag{31}$$

The power computed was converted to dimensionless parameter as follows:
The dimensionless extrusion pressure P/σ_0 is given by

$$\frac{P}{\sigma_0} = \frac{P^*}{A_0 V_0 \sigma_0}. \tag{32}$$

The die land length (x) is also reduced to the relative die land length by dividing by original billet diameter (x/D_0).

2.4. Computational method

When the geometry of exit cross-section or the die is given, the surface of the die can then be known explicitly. By performing, the necessary differentiations and integrations on shapes of the die surface functions, the velocities field's Eqs. (6)–(8) and strain rates Eqs. (9)–(14) were derived.

The area and volume integrals of Eq. (31) were performed, using the Gaussian quadrature integration techniques by transforming the polynomial variable by

$$\phi(x_i) = \frac{(b-a)z_i + (b-a)}{2}, \tag{33}$$

where a and b are, respectively, the upper and lower limits of integrations of the zone of die surface giving.

The area integrals of the friction losses, W_f, and shear losses, W_s, into

$$\iint \psi(\eta, \varepsilon)\,\mathrm{d}\eta \mathrm{d}\varepsilon = \sum_{i=1} \sum_{j=i} W_p W_j \psi(\eta_i, \varepsilon_j)\,\mathrm{d}\eta\,\mathrm{d}\varepsilon, \tag{34}$$

where $\psi(\eta_i \varepsilon_j)$ is the resultant velocity field and $W_p W_j$ are assigned weightings and for volume integrals of the internal powers of deformation (W_i) is given as

$$\iiint \psi(\eta, \varepsilon, G)\,\mathrm{d}\eta\,\mathrm{d}\varepsilon\,\mathrm{d}G = \sum_{i=1} \sum_{j=1} \sum_{k=1} \psi(\eta_i, \varepsilon_j, G_k)\,\mathrm{d}v, \tag{35}$$

where $\psi(\eta_i, \varepsilon_j, G_k)$ is the resultant strain and volume under deformation. A computer program written in C++ language was used [23] to evaluate various components of Eq. (31) to determine dimensionless extrusion pressure P/σ_0.

3. Results and discussions

3.1. Relative extrusion pressure, (P/Y), determinations

3.1.1. Rectangular and square die openings

The relative extrusion pressures, P/Y, versus die lengths, l/r_0, for rectangle ($b{:}a = 2{:}1$) and square sections are shown in Figs. 6 and 7, respectively, for varying die land lengths indicated. It may be seen that for a given die land length, x, the relative extrusion pressures, P/Y, decrease with increasing relative die lengths, l/r_0, until a minimum relative length is reached, beyond this minimum relative length, relative extrusion pressures start to increase again. The normalized extrusion pressure, $P_{\min}/Y$, that corresponds to this minimum relative extrusion pressure gives the optimal extrusion pressure, $P_{\min}/Y$, that is required to extrude under a given die land length for a given percentage reduction in area under

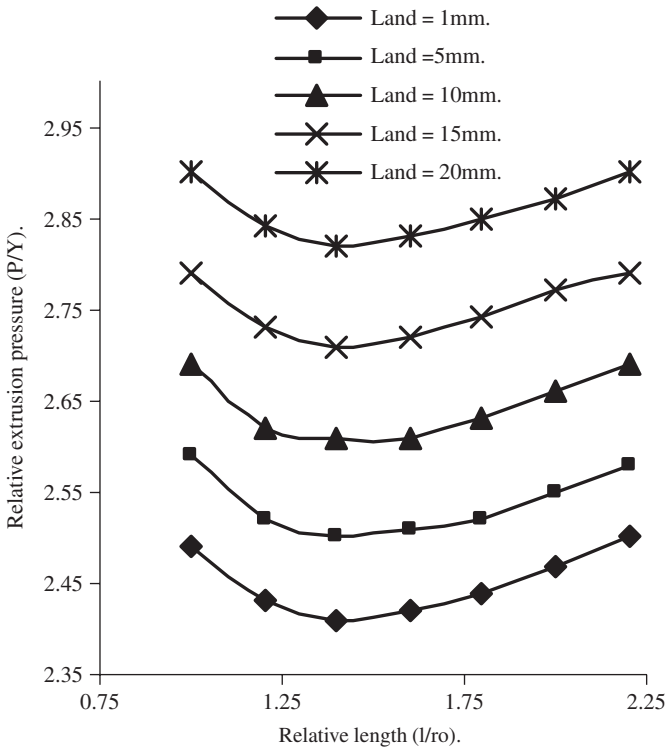

Fig. 6. Effect of die land lengths on the extrusion pressures of a rectangular die opening of die reduction in area of 58%.

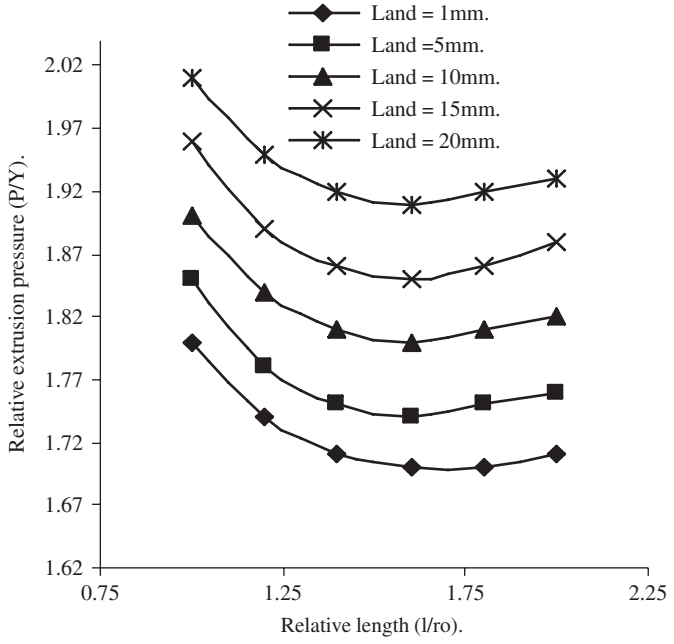

Fig. 7. Effect of die land lengths on the extrusion pressures of a square die opening of die reduction in area of 58%.

consideration. It can be seen that, by increasing the die land lengths will produce various optimal relative extrusion pressures irrespective of die opening's geometry (see Figs. 6 and 7). Also, from Figs. 6 and 7 using the same friction coefficient of 0.065 and percentage reduction in area of 58, the optimal relative die lengths are found to occur at the same points i.e. $l/r_0 = 1.4$ and 1.6 for rectangular and square die openings, respectively, for all various die land lengths considered. This is in close agreement with Chitkara and Celik [2] findings in their analytical models on the extrusion of T-section shape that for a particular friction factor, the optimal die length changes only slightly provided the reduction in cross-section area was either the same or was close to each other.

For other varying percentage reductions in area, R say 69% and 76%, the optimal relative die lengths are found to occur at $l/r_0 = 1.5$ and 1.6, respectively for square die opening and at the same values of reduction in areas of 69% and 76%, the optimal relative die lengths are $l/r_0 = 1.5$ and 1.6, respectively for rectangular die opening.

By repeating similar procedures, the optimum extrusion pressures are determined for other varying die land lengths, say 1, 5 mm, etc. at a given percentage reduction in area for respective rectangular and square sections openings of Figs. 6 and 7. The whole procedures are repeated at varying die land lengths and percentages reductions in area to give Figs. 12 and 13 for respective rectangular and square die openings.

3.1.2. I- and T-sections openings

Fig. 8 shows a typical plot of relative extrusion pressures, P/Y, versus relative die length, l/r_0, computed for different area ratios, A_2/A_1, using a reduction in area of 58% for the I-shaped section at a given die land length of 15 mm. It can be seen from these figures that, for a given area ratio, the relative extrusion pressures, P/Y, decreases with increasing relative die lengths, l/r_0, to a minimum value at a known relative length. Beyond this relative length, increasing the relative die lengths, l/r_0, lead to increasing relative extrusion pressures, P/Y. The relative die length that produced minimum relative extrusion pressures, P_{min}/Y, gives the optimal relative extrusion pressure for a given area ratio and for a given die land length of 15 mm. Fig. 9 shows the results of relative extrusion pressure, P/Y, versus relative die length, l/r_0 computed for different area ratios, using reductions in area of 58% for the T-shaped section at a given die land length of 15 mm. It can be seen from this figure also that, for a given area ratio, the relative extrusion pressure, P/Y, decreases with increasing relative die lengths (l/r_0) to a minimum value at a known relative length. Beyond this relative length, increasing the relative die lengths (l/r_0) lead to increasing relative extrusion pressures, P/Y. The relative die length that produced minimum relative extrusion pressure P_{min}/Y, gives the optimal relative extrusion pressure or normalized extrusion pressure, P_{min}/Y, at a given area ratio $A_2/A_1 = 0.45$ for the given die land length of 15 mm considered.

Variation of optimal relative extrusion pressures, P_{min}/Y obtained from Fig. 8 for various area ratios indicated plotted against area ratios (A_2/A_1) at a given typical die land of 15 mm and other die land lengths for a given reduction in area of 58% for I-shaped section is shown in Fig. 10. This figure reveals that, optimal relative extrusion pressures decrease with increasing area ratios, until a minimum value is reached at a known area ratio. Beyond this area ratio, increasing area ratio causes increasing optimal relative extrusion pressures obtained from the relative die length (l/r_0) of Fig. 8. From Fig. 10 the correct relative extrusion pressure, P'/Y, that corresponds to a minimum value obtained at a known area ratio gives the correct optimal extrusion pressure or correct normalized extrusion pressure, P'/Y, to extrude lead billet through I-die opening at a given percentage reduction in area of 58% and at a given die land length of 15 mm. Variation of optimal relative extrusion pressures, P_{min}/Y, obtained from Fig. 9 for various area ratios indicated plotted against area ratio, A_2/A_1, at different die land lengths using a given reduction in area of 58% for T-shaped section (see Fig. 11). Fig. 11 reveals that,

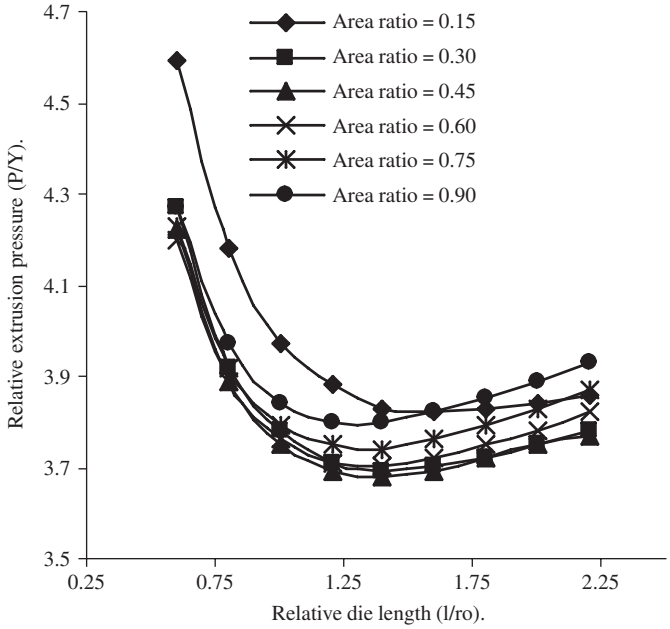

Fig. 8. Typical effects of area ratios on the extrusion pressures of I-die opening geometry at a given die reduction in area of 58% and at constant die land length of 15 mm

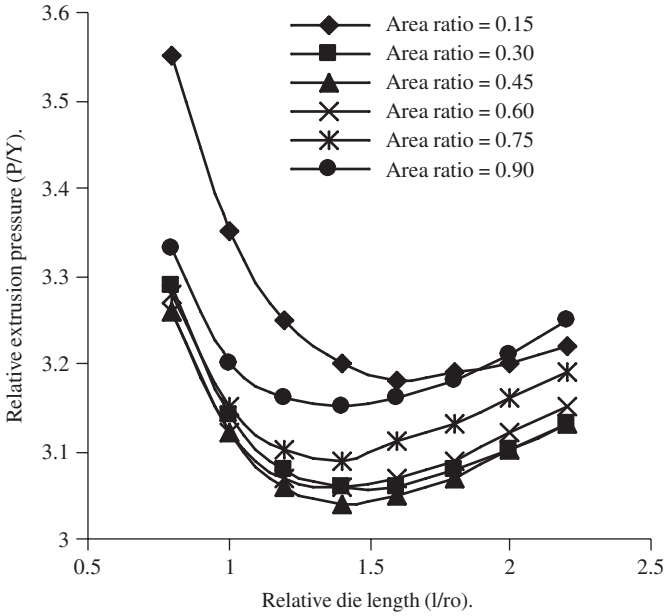

Fig. 9. Typical effects of area ratios on the extrusion pressures of I-die opening geometry at a given die reduction in area of 58% and at constant die land length of 15 mm.

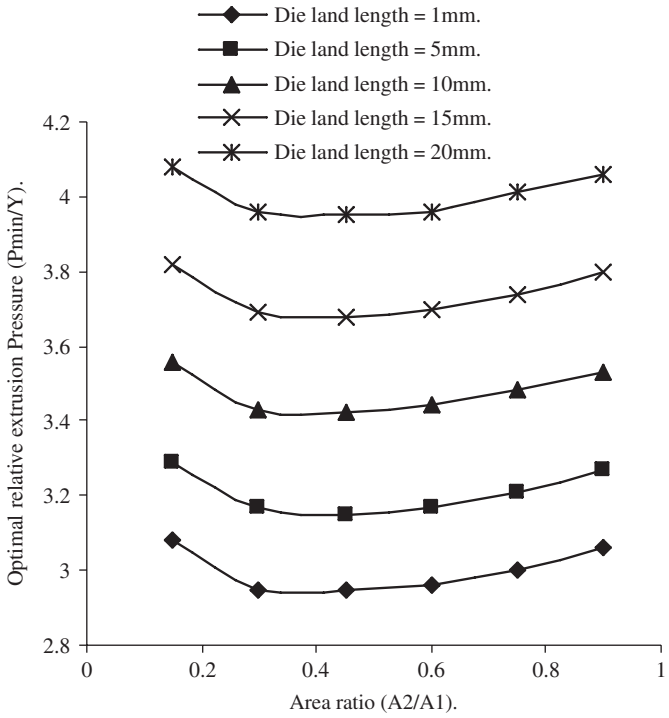

Fig. 10. Effects of die land lengths on the extrusion pressures of I-die opening at a given die reduction in area of 58%.

optimal relative extrusion pressures, $P_{\min}/Y$, decrease with increasing area ratios, until a minimum value is reached at a known area ratio. Beyond this area ratio, increasing area ratios cause increasing optimal relative extrusion pressures $P_{\min}/Y$ obtained from the relative die length, l/r_0, for a given die land length of say 15 mm of Fig. 9. From Fig. 11 the correct optimal relative extrusion pressure, $P_{\min}/Y$, that corresponds to a minimum value obtained at a known area ratio of $A_2/A_1 = 0.45$, for a given die land of 15 mm gives the correct optimal extrusion pressure or correct normalized extrusion pressures, P'/Y, to extrude lead billet through T-die opening at a given percentage reduction in area (i.e. 58%). Using Figs. 8 and 9 for intermediate analyses for the extrusions of I- and T-section shapes, the optimal relative die lengths at various area ratios A_2/A_1, considered are found to vary with area ratios for a given 58% reduction in area (Table 1) (see Table 2). From Figs. 10 and 11, the optimal relative extrusion pressures, $P_{\min}/Y$, for I- and T-shaped sections, respectively,

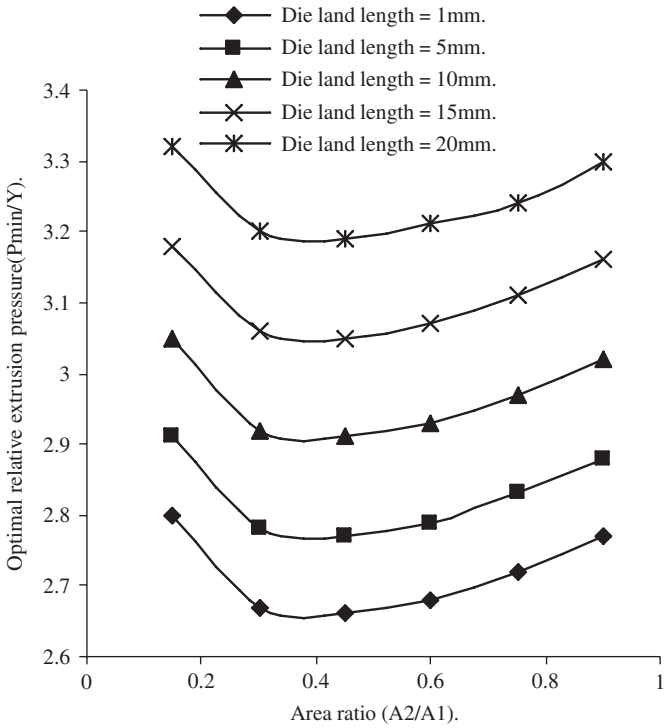

Fig. 11. Effects of die land lengths on the extrusion pressures of T-die opening at a given die reduction in area of 58%.

Table 1
Die land extrusion pressure contributions, $\Delta P_o/Y$, at various percentages reductions in area for various die openings profiles

Die opening geometry	%reduction in area, R	Extrapolated extrusion pressure (P_o/Y) MN/m^2	Die land length contribution to extrusion pressure $\Delta P_o/Y$					Experimental/Theoretical Values in literature
			1 mm	5 mm	10 mm	15 mm	20 mm	
Square	50	1.43	0.01	0.04	0.09	0.12	0.18	1.48 [24]
	58	1.69	0.01	0.05	0.11	0.16	0.22	
	69	2.06	0.01	0.07	0.13	0.2	0.27	
	76	2.31	0.01	0.07	0.14	0.21	0.29	
Circular	58	1.80	0.01	0.06	0.12	0.18	0.24	1.81 [23]
Rectangular	58	2.39	0.02	0.11	0.22	0.32	0.43	2.42 [5]
	69	2.61	0.02	0.12	0.25	0.38	0.51	
	76	2.76	0.03	0.14	0.28	0.42	0.56	
T-shaped	58	2.63	0.03	0.14	0.28	0.41	0.55	
	70	2.92	0.06	0.27	0.53	0.80	1.07	2.90 [4]
	76	2.99	0.9	0.42	0.84	1.25	1.67	
I-shaped	58	2.89	0.06	0.26	0.53	0.79	1.06	
	69	3.11	0.09	0.44	0.87	1.30	1.74	3.10 [13]
	76	3.27	0.12	0.60	1.20	1.80	2.40	3.82 [13]

are found to occur at the same area ratios of $A_2/A_1 = 0.45$ for a given percentage reduction of 58. However, it can be further seen from Table 2, that the optimal relative extrusion pressures, $P_{\min}/Y$, for I- and T-shaped sections, occur at the same optimal area ratios, although the values of such area ratios are found to vary with percentages reductions in areas (see Table 2).

Similar procedures used to obtain the normalized extrusion pressure, P'/Y, for a given die land length of say 15 mm at a given percentage reductions in area for I- and T-sections are repeated for other die land lengths of 1, 5 mm, etc. for 58% reduction in area as given, respectively, by Figs. 10 and 11.

Table 2
Optimal relative die lengths, area ratios and optimal relative extrusion pressures with varying percentages reductions in areas for I- and T-shaped sections at die land length of 15 mm

%reduction in area	Area ratio A_2/A_1	Optimal relative die length (l/r_o) (I-section)	Optimal relative die length (l/r_o) (T-section)	Optimal area ratios for optimal relative extrusion pressure (P_{min}/Y)
58	0.15	1.6	1.6	I-section $A_2/A_1 = 0.45$
	0.30	1.4	1.6	T-section $A_2/A_1 = 0.45$
	0.45	1.4	1.4	
	0.60	1.4	1.4	
	0.75	1.4	1.4	
	0.90	1.4	1.4	
69	0.15	1.6	1.8	I-section $A_2/A_1 = 0.375$
	0.30	1.5	1.6	T-section $A_2/A_1 = 0.375$
	0.45	1.4	1.6	
	0.60	1.4	1.4	
	0.75	1.4	1.4	
	0.90	1.4	1.4	
76	0.15	1.6	1.8	I-section $A_2/A_1 = 0.30$
	0.30	1.5	1.6	T-section $A_2/A_1 = 0.30$
	0.45	1.4	1.6	
	0.60	1.4	1.6	
	0.75	1.4	1.4	
	0.90	1.4	1.4	

The whole procedures are again repeated for other percentages reductions say 58%, 69% in area with varying die land lengths to give Figs. 14 and 15 for I- and T-die openings, respectively.

3.2. Variation of normalized extrusion pressure with relative die land length

3.2.1. Square and rectangular die openings

Figs. 12 and 13 show the theoretical plots of normalized extrusion pressure, P'/Y versus normalized or relative die land lengths, x/D_o, for respective rectangular and square sections openings computed for varying percentages reductions in area indicated. It can be seen that, increasing the percentages reductions in area leads to increasing normalized extrusion pressures P'/Y for any given die land lengths and also that, increasing die land lengths leads to increasing normalized extrusion pressure at any given percentage reduction in area investigated.

3.2.2. I- and T-section openings

Figs. 14 and 15 show plots of the correct normalized extrusion pressures, P'/Y, against normalized die land lengths at varying die reductions in area indicated for I- and T-shaped sections openings, respectively. These figures indicate that the correct normalized extrusion pressure is found to increase with increasing percentage die reduction in area at any given die land lengths and also with increasing die land lengths at any given percentage reduction in area. It can be seen that the higher the percentage reduction in area, the higher the extrusion pressure to extrude T- and I-shaped sections. Also, the higher the die land length, the higher the extrusion pressures rise in extruding I- and T-shaped sections. The effect of percentage reduction in area and the die land length is seen to be more pronounced in I-shaped section than in T-shaped section. This is in agreement with the experimental work of Chitkara and Adeyemi [13] on the effect of percentage reduction in area on the extrusion pressures of I- and T-shaped die openings with extrusion pressures of I-shaped section being higher than for T-shaped section opening.

3.2.3. Die land length and die geometries extrusion pressure contributions, $\Delta P_0/Y$, Determination

Extrapolating each plot of Figs. 12–15 to intercept the extrusion pressure axis, give the values of normalized extrusion pressure P_0/Y corresponding to zero die land length for each reduction in area indicated. For each given reduction in area, this value subtracted from the correct normalized extrusion pressure value P'/Y obtained for various die land lengths gives the extrusion pressure contribution of each die land length to the extrusion pressure as $\Delta P_o/Y = (P' - P_o)/Y$. The dimensionless die land length extrusion pressure contributions, $\Delta P_o/Y$, is seen to generally increase with increase die land lengths and also increase with increase percentages reductions in area (see Table 1) for all die openings geometries investigated. It can be seen that, generally, die land lengths contribute significantly to the extrusion pressures for all die

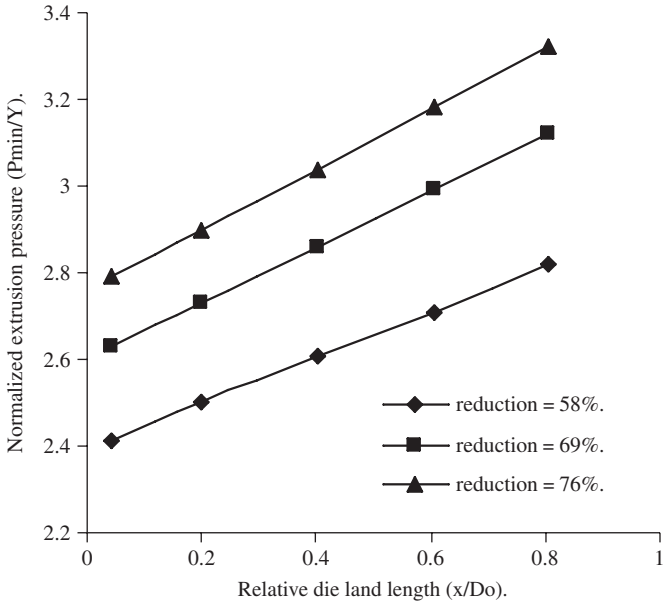

Fig. 12. Effect of percentages reduction in area on the normalized extrusion pressures in the extrusion of a rectangular product over relative die land lengths.

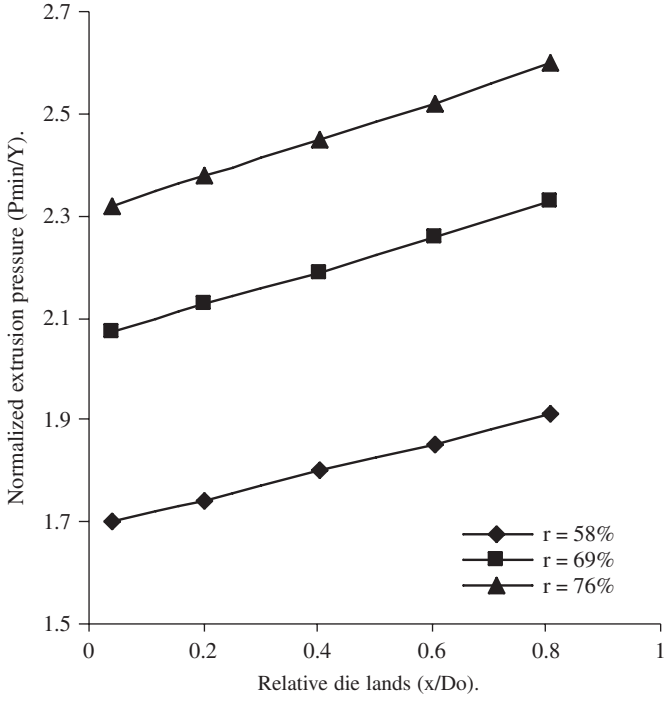

Fig. 13. Effect of percentages reduction in area on the normalized extrusion pressures of a square product over relative die land lengths.

openings geometries and more especially at higher die reductions for particular I- and T-die opening geometries. Higher perimeters of these geometries coupled with higher frictional effects may possibly account for the higher contributions of die land lengths to the total extrusion pressures (see Table 1).

Fig. 16 shows the plot of the correct relative extrusion pressure, P/Y versus increasing relative die land lengths at a given die reduction of 58% for circular, rectangle, square, T and I-sections shaped die openings. The I-shaped section die opening gives the highest extrusion pressure, followed by T-shaped section, rectangular, circular-shaped die openings with square section die opening, giving the least extrusion pressure for the given 58% die reduction at any given die land lengths.

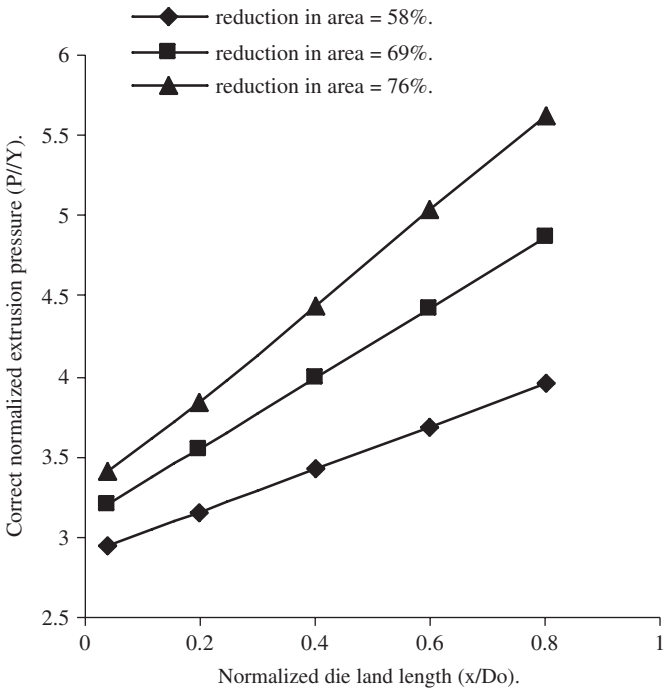

Fig. 14. Effects of die reduction in areas on the correct normalized extrusion pressures of I-die opening.

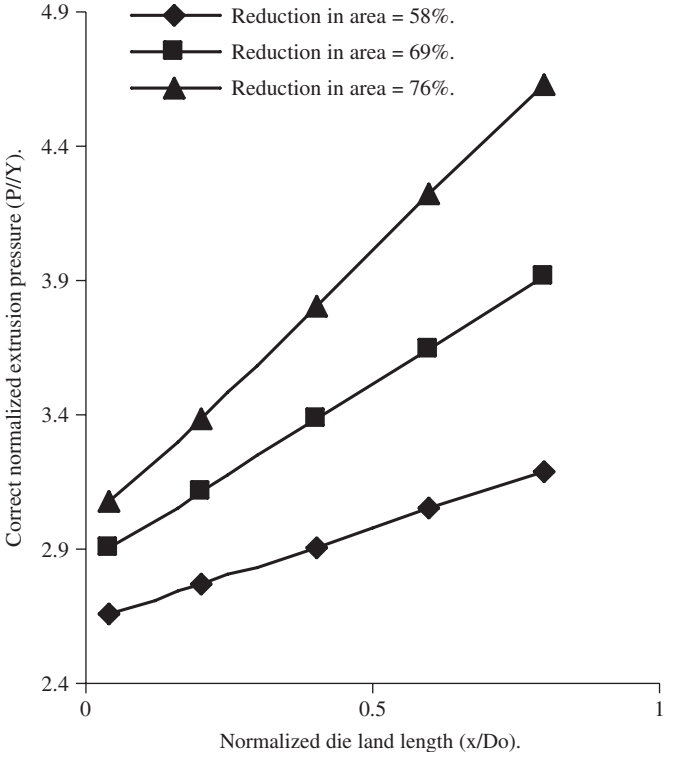

Fig. 15. Effects of die reduction in areas on the correct normalized extrusion pressures of T-die opening.

4. Conclusions

Upper bound analysis to take into account the die land lengths on the extrusion pressure is formulated and used to solve the extrusion pressures for complex extruded sections such as square, rectangular, I- and T-shaped sections with power of

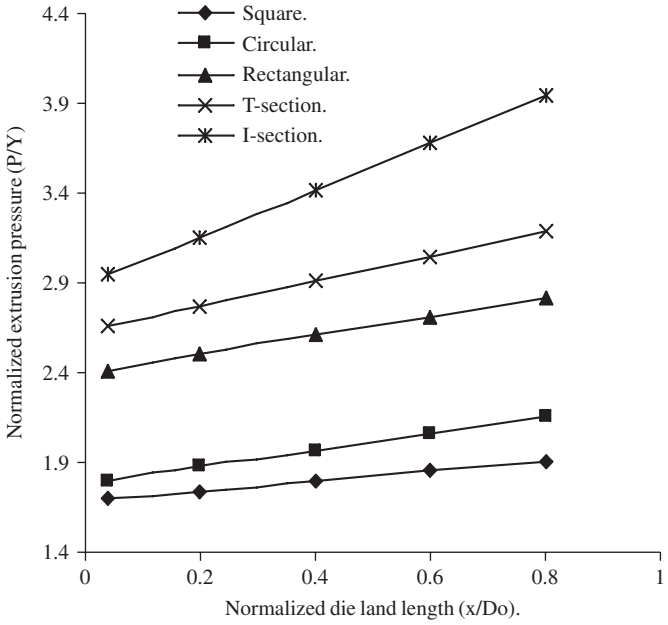

Fig. 16. Effects of die openings geometries on the normalized extrusion pressures at a given die reduction in area of 58%.

deformation due to ironing effect at die land included. The extrusion pressure contributions due to the die land evaluated theoretically for shaped sections considered are found to increase with die land lengths for any given percentage reduction and also increase with increasing percentage die reductions at any given die land length. The effect of die land length on the extrusion pressure increases with increasing complexity of die openings geometry with I-shaped section giving the highest extrusion pressure followed by T-shaped section, rectangular, circular-shaped die openings with square section die opening, giving the least extrusion pressure for any die reductions at any given die land lengths.

Acknowledgment

One of the authors, J.S. Ajiboye, is grateful to the University of Lagos, Lagos, Nigeria for their financial support during the research work. We also thank the Authorities of Kwara Polytechnics, Ilorin and Department of Mechanical Engineering, University of Ilorin, for allowing us the use of their laboratories equipment. I also, appreciate the assistance rendered by Mr. Saka Saidu, a Technologist with Kwara State Polytechnics.

Reference

[1] Chitkara NR, CeliK KFA. Generalized CAD/CAM solution to the three-dimensional off-centric extrusion of shaped sections: analysis. International Journal of Mechanical Sciences 2000;42:295–320.
[2] Chitkara NR, Celik KFA. Extrusion of non-symmetric T-shaped sections on analysis and some experiments. International Journal of Mechanical Sciences 2001;43:2961–87.
[3] Chitkara NR, Yohngjo Kim. An analysis of external spline gear forming by an upper bound energy method. International Journal of Mechanical Sciences 1996;38(7):777–89.
[4] Chitkara NR, Yohngjo Kim. Upper bound analysis of near-net shaped forging of gear coupling form. International Journal of Mechanical Sciences 1996;38(7):791–803.
[5] Wu CW, Hsu RO. Theoretical analysis of extrusion of rectangular, hexagonal and octagonal composite clad rods. International Journal Mechanical Sciences 2000;42:473–86.
[6] Choi JC, Choi Y, Hur KD, Kim CH. A study on the forging of spur gears. International Journal of Mechanical Sciences 1996;18(12):1333–47.
[7] Kar PK, Das NS. Upper bound analysis of extrusion of I-section bars from square and rectangular billets through square dies. International Journal of Mechanical Science 1997;39(8):925–34.
[8] Celik KFA, Chitkara NR. Application of an upper bound method to off-centric extrusion of square sections, analysis and experiments. International Journal of Mechanical Sciences 2000;42:321–45.
[9] Chitkara NR, Bhutta MA. Computer simulation to predict stresses, working pressures and deformation modes in incremental forging of spur gear forms. International Journal of Mechanical Science 1996;38(8–9):871–89.
[10] Bae, et al. Upper-bound analysis of square-die forward extrusion. Journal of Materials Processing Technology 1996;62:242–8.
[11] Maity, et al. A class of upper-bound solutions for the extrusion of square shapes from square billets through curved dies. Journal of Materials Processing Technology 1996;62:185–90.

[12] Qamar, et al. , Variation of pressure with ram speed and die profile in hot extrusion of Auminum-6063. Materials and Manufacturing processes 2004;19(3):391–405.
[13] Chitkara NR, Adeyemi, MB. Working pressure and deformation modes in forward extrusion of I and T shaped sections from square slugs.In: 18th international. M. T. D. R Conference. Proceedings, imperial college of science and Tech. London 1977.p. 289–301.
[14] MacLellan GDS. A critical survey of wire-drawing theory. Journal of the British Iron and Steel Institute 1948;158:347–56.
[15] Wistreich JG. Investigation of the mechanics of wire drawing. Proceedings of the Institution of Mechanical Engineers 1955;169:654–65.
[16] Hoffman O, Sachs G. Theory of plasticity. New York, N.Y.: McGraw-Hill .; 1953 176–180.
[17] Yang CT. On the mechanics of wire drawing. Transactions of the ASME— Journal of Engineering for Industry 1961:523–30.
[18] Kiuchi M, Kish H, Ishikawa M. Study on nonsymmetric extrusion and drawing. In: 22nd Proceedings of the Conference.1981.p. 523–32.Int Journal Mach Tool Design Research.
[19] Nanhai, et al. Numerical design of die land for shape extrusion. Journal of Material Processing Technology 2000;101:81–4.
[20] Ajiboye JS, Adeyemi MB. Computer modeling of the effects of billets and extruded symmetric section shapes in the forward extrusion. Nigerian Journal of Technical Education 1999;16(1):1–14.
[21] Avitzur B. Analysis of wire drawing and extrusion through conical dies of small cone angle. Transactions of the ASME— Journal of Engineering for Industry 1963:89–96.
[22] Ajiboye JS, Adeyemi MB. Effects of die land on the cold extrusion of lead alloy. Journal of Materials Processing Technology 2006;171:428–36.
[23] Ajiboye JS. Extrusion pressure and temperature changes during forward extrusion process. PhD thesis. Department of Mechanical Engineering, University of Ilorin, Ilorin, Nigeria 2006.
[24] Onawola OO, Adeyemi MB. Warm compression and extrusion tests of aluminum. Journal of Materials Processing Technology 2005;136:7–11.